FRACTURE BEHAVIOR OF CEMENTED CARBIDES: A FRACTURE MECHANICS ANALYSIS

L. Llanes[1], Y. Torres[1], B. Casas[1], D. Casellas[1], F. Marimon[2], F, Roure[2] and M. Anglada[1]

[1] Departament de Ciència dels Materials i Enginyeria Metal·lúrgica,
ETSEIB, Universitat Politècnica de Catalunya, 08028 Barcelona, SPAIN
[2] Departament de Resistència de Materials i Estructures a l'Enginyeria,
ETSEIB, Universitat Politècnica de Catalunya, 08028 Barcelona, SPAIN

ABSTRACT

The fracture behavior of WC-Co hardmetals with different microstructures was studied. Microstructural variables included cobalt volume fraction and carbide grain size. Experimental characterization was conducted in terms of fracture toughness, flexural strength and fractography. The experimental findings were combined with a theoretical fracture mechanics analysis, including crack configuration modeling, in order to estimate critical flaw size. In doing so, processing flaws (e.g. pores, carbide agglomerates, etc.) were considered as a localized defect, acting as a stress concentrator, plus a circumferential crack. The mean carbide grain size was taken as the microstructural scale associated with the length of this crack, a key variable within the predictive model. Such an assumption is sustained by previous tailoring of the model using the strength, toughness and fractographic experimental data. A quite satisfactory concordance between estimated and experimentally determined values for the critical flaw size is finally attained.

INTRODUCTION

The implementation of fracture mechanical thinking to rationalize the fracture behavior of ceramics and other brittle-like materials is well established. The fact that rupture in these materials normally initiates at pre-existing defects sustains design methodologies based on linear elastic fracture mechanics (LEFM), according to generic relationships of type:

$$K_{IC} = Y \sigma (\pi a)^{1/2} \quad (1)$$

where K_{IC} is the material toughness, in terms of prevention of crack extension; σ is the applied nominal stress; Y is a geometrical factor, function of crack shape and loading mode; and a is the size of the pre-existing flaw. On the other hand, in applying LEFM criteria it is common to assume fracture-controlling flaws as if they were simple circular cracks. Although such a practice may be useful enough, within Eqn. 1, either to monitor a design or to aid in certifying structural components involving brittle materials [1], it does not seem to be the most appropriate alternative for an accurate description of the fracture behavior of these materials.

Detailed scrutiny of fracture surfaces in brittle-like materials clearly point out that failure origins are usually defects with aspect quite different from that of simple circular cracks, e.g. pores, grain clusters, inclusions, etc. [2-4]. Hence, reliable procedures attempting to assess size, geometry and type of critical flaws should include particular features associated with real configurations of the experimentally observed defects. Within this scope, one interesting approach is the consideration of the whole flaw as a localized defect (crack) in combination with the stress concentration around the discerned flaw (e.g. a pore) [5,6]. This approach will be addressed here for analyzing the fracture behavior of WC-Co cemented carbides with different microstructures. In doing so, experimental data comprising fracture strength, fracture toughness and fracture-controlling flaw characteristics, the latter discriminated by means of scanning electron microscopy, are first attained. Then, the referred fracture model is tailored, in terms of effective crack length scale, using the collected experimental data. Finally, estimated values for the critical flaw size, from predictive fracture mechanics models based on different crack configurations, are compared and discussed with respect to those experimentally determined.

EXPERIMENTAL PROCEDURE

The materials studied were commercial WC-Co hardmetals provided by DURIT Metalurgia Portuguesa do Tungsténio, Lda. Five grades corresponding to selected combinations of two mean grain sizes of carbide, d_{WC} (0.8 μm and 2.5 μm), and three volume fractions of cobalt, V_{Co} (about 10, 16 and 27 $\%_{vol}$), were investigated. The identification code, following the nomenclature used by the supplier, and the key microstructural parameters of each grade are given in Table 1. Microstructural characterization includes values for carbide contiguity (C_{WC}) and cobalt binder thickness (λ_{Co}), as estimated from empirical relationships given in the literature [7], but refined to account for d_{WC} variations [8]. Micrographs of two of the WC-Co composites studied are presented in Figure 1.

TABLE 1
NOMENCLATURE AND MICROSTRUCTURAL DATA

Grade	V_{Co} ($\%_{vol}$)	d_{WC} (μm)	C_{WC}	λ_{Co} (μm)
GD03	10.2	0.8	0.66	0.3
GD10	10.1	2.5	0.41	0.5
GD13	16.3	0.8	0.44	0.3
GD20	16.4	2.5	0.27	0.7
GD40	27.4	2.5	0.17	1.1

Fracture resistance was evaluated in terms of flexural strength. Prismatic specimens with 45x4x3 mm dimensions and chamfered edges were used. Tensile surfaces for the flexure tests were ground and polished. Flexural strength measurement was performed using a standard 20x40 mm fully articulating four-point fixture. At least six samples were tested for each grade.

Fracture toughness was assessed using the single edge notched beam (SENB) method. The sample geometry employed was a rectangular bar of 45x10x5 mm dimensions. The effective evaluation of fracture toughness using fracture mechanics requires the suitability of a procedure for introducing a sharp pre-crack into the sample. In this study it was achieved through application of cyclic compressive loads to a SENB specimen, followed by stable crack growth under far-field tensile stresses. The latter step was conducted to relieve residual stresses induced during the previous cyclic compression [9]. A detailed description of the pre-cracking procedure used has been reported elsewhere [10]. Fracture toughness values were determined by testing the pre-cracked SENB samples to failure and using the stress intensity factor given by Tada *et al.* [11]. At least three specimens were evaluated for each material.

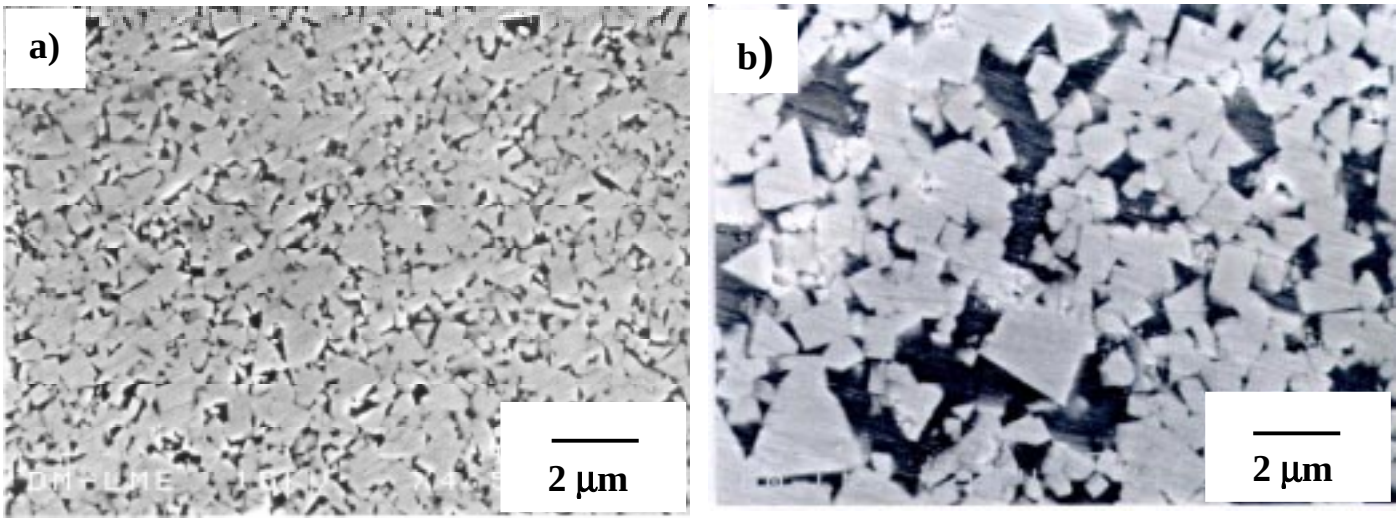

Figure 1: Microstructures of **(a)** GD13 and **(b)** GD40 WC-Co grades.

Fracture surfaces for all the tested samples were inspected through scanning electron microscopy (SEM). For each sample, possible fracture initiation sites were first traced back, at low magnification, from sequential sets of fracture surface markings. Particular areas of interest were then examined at higher magnification and, where it was possible, size, geometry and type of the strength-limiting flaw were measured and discerned.

RESULTS AND DISCUSSION

Flexural strength (σ_r) and fracture toughness for each hardmetal grade studied are given in Table 2. As it is well known from the literature (extended data compilations may be found in Refs. [8,12]), they are strongly dependent upon volume fraction and free mean path of the cobalt binder, and the contiguity and mean size of the tungsten carbide grains. However, consistent relationships may only be established between fracture toughness and microstructure, indicating the intrinsic character of this fracture parameter as a material property. Combined carbide grain size and cobalt content effects are rationalized through particular two-phase microstructural parameters such as carbide contiguity and binder thickness. As a result, fracture toughness is found to exhibit a rising trend with increasing cobalt mean free path (and decreasing carbide contiguity). On the other hand, flexural strength variations among the different grades are speculated to be an indirect consequence of microstructural effects on fracture toughness and critical flaw size, the latter intimately associated with the processing stages.

An extended fractographic examination of the broken specimens indicated that they invariably failed from subsurface origins. These fracture initiation sites were identified as processing heterogeneities: pores, binderless carbide clusters and discrete WC-Co agglomerates. Two examples of failure controlling defects

TABLE 2
FRACTURE PARAMETERS: STRENGTH AND TOUGHNESS

Grade	σ_r (MPa)	K_{IC} (MPa$\sqrt{m}$)	K_{IC}/σ_r ($\sqrt{m}$)
GD03	1676	7.5	0.0045
GD10	2094	10.3	0.0049
GD13	2742	9.2	0.0034
GD20	1813	10.5	0.0058
GD40	2629	16.0	0.0061

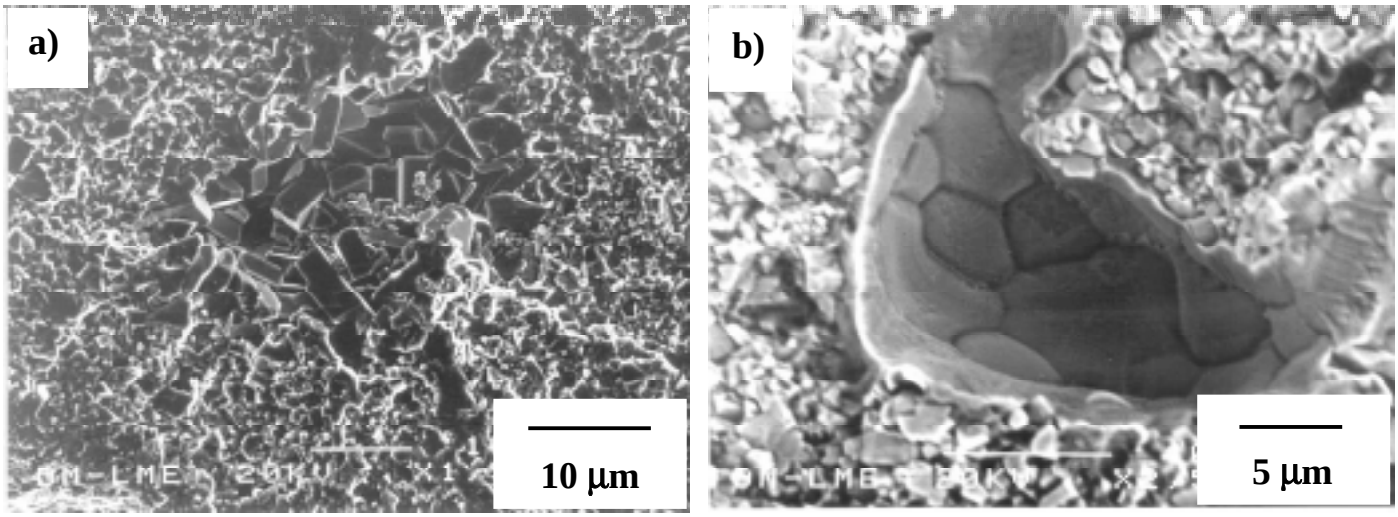

Figure 2: Examples of typical fracture origins in WC-Co hardmetals:
(a) carbide clusters (GD20) and **(b)** pores (GD40).

are shown in Figure 2. Quantitative analysis was conducted to precise the dimensions of the strength degrading defects. Critical flaw size ranges, from direct SEM measurements, for each hardmetal grade are given in Table 3. They are expressed in terms of 2a, where a is the radius of a circular flaw whose cross-sectional area is equivalent to that of the rather irregular-shaped defects experimentally observed.

Following the above experimental findings, the fracture behavior of WC-Co cemented carbides will now be analyzed by recourse to a simplified fracture mechanics model. It is based on the consideration of flaws as consisting of a (spherical) defect that acts as a stress concentrator plus an equatorial crack around it. The corresponding schematic representation, including the nomenclature used in this study, is given in Figure 3a. The length of this circumferential crack is an important variable in the model because it sets the value of applied stress intensity factor around the spherical defect. As it has been previously stated for other polycrystalline ceramics [13-16], a correct approximation of the size of this crack requires an exhaustive evaluation of the microstructure at the fracture origin. For the particular case of cemented carbides, the intrinsic fine microstructure of these materials makes difficult to clearly determine the extension, and even the existence, of such a crack. However, they may be speculated to exist once residual stresses at carbide-binder interfaces, as a consequence of significant thermal contraction mismatch induced by the large difference between the coefficients of thermal expansion of WC and Co, are accounted. About the crack extension, it is expected to be intimately associated with particular microstructural features [3,17,18]. Information aiming to discern the appropriate microstructural scale of the crack length, within the model just described, may be attained through comparison of experimental and estimated values for the flaw size.

TABLE 3
EXPERIMENTAL CRITICAL FLAW SIZE AND ESTIMATED CIRCUMFERENTIAL CRACK PARAMETERS

Grade	$(2a)_{experimental}$ (μm)	$(c/R)_{estimated}$	$c_{estimated}$ (μm)
GD03	12-32	0.15	2.0
GD10	15-38	0.30	3.0
GD13	8-14	0.40	2.0
GD20	14-34	0.30	5.0
GD40	30-42	0.40	6.5

In order to assess the value of the applied stress intensity factor around the observed processing heterogeneities, it is assumed that all of them, independent of their specific nature, can be treated as internal spherical pores with circumferential cracks. Such an assumption is partly sustained by the experimental fact that physical separation between carbide clusters or material agglomerates and the hardmetal matrix was commonly revealed. Figure 3b displays, in a 3-D plot, the normalized applied stress intensity factor (K/σ) for the referred pore-crack configuration [5,19,20] as a function of normalized crack length (c/R) and defect size (2R).

a) **b)**

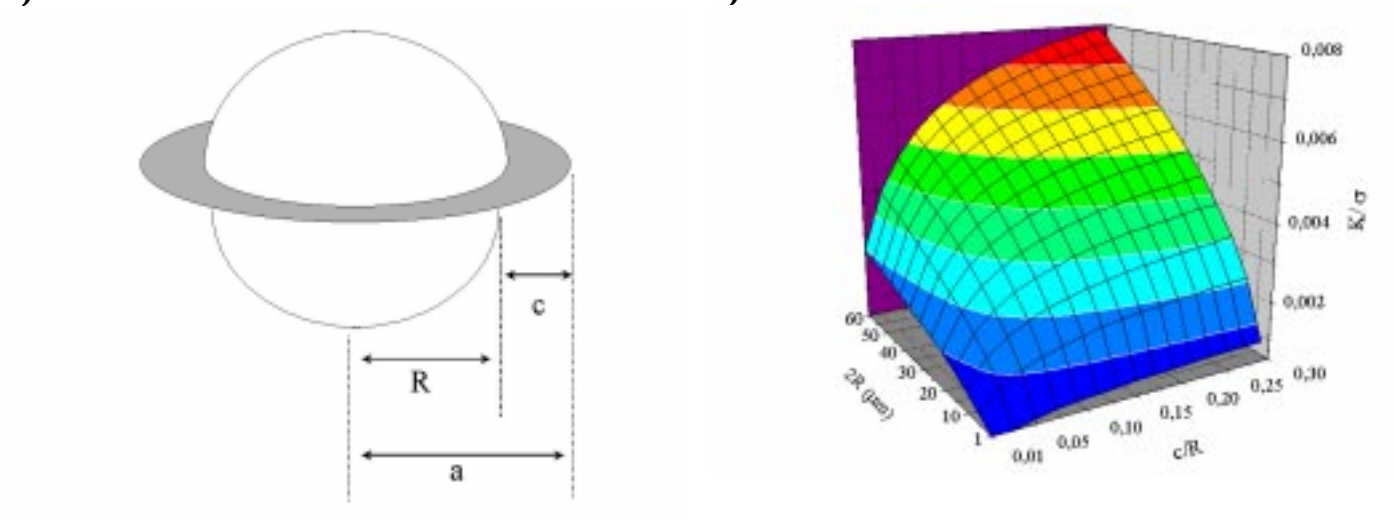

Figure 3: (a) Schematic representation and associated nomeclature of circumferential crack emanating from a spherical pore; **(b)** normalized stress intensity factor (K/σ) as a function of normalized crack length (c/R) and defect size (2R).

Effective c/R ratios for each cemented carbide grade may be estimated from Figure 3b, once the experimental values of flexural strength, fracture toughness and critical flaw size (listed in Tables 2 and 3) are incorporated as inputs to calibrate the predictive fracture mechanics model. The best-fitting results, in terms of both c/R and c, are also included in Table 3. It is appreciated that the microstructural scale of the crack length is the corresponding mean carbide size. Specific flaw size estimations using predictive fracture mechanics models based on assuming critical flaws as: 1) simple circular cracks, i.e. with $c/R \rightarrow \infty$ and $Y=2/\pi$, and 2) circumferential cracks of length twice the mean carbide grain size, are given in Table 4. The results of the former approach are significantly above the range of experimental flaw size for most of the hardmetal grades. On the other hand, the latter approach yield estimated values that are much closer to those determined experimentally, pointing out the appropriateness of considering the critical flaw as consisting of a stress concentrating defect plus an equatorial crack for describing the fracture behavior of cemented carbides.

TABLE 4

ESTIMATED CRITICAL FLAW SIZE USING DIFFERENT PREDICTIVE FRACTURE MECHANICS MODELS

	$(2a)_{estimated}$ (μm)	
Grade	$c/R \rightarrow \infty$, $c = a$, $Y = 2/\pi$	$0 < c/R < \infty$, $c = 2d_{WC}$, $Y = f(c/R)$
GD03	32	37
GD10	38	30
GD13	18	15
GD20	52	42
GD40	58	47

SUMMARY

The fracture behavior of WC-Co cemented carbides has been satisfactorily rationalized through a fracture mechanics analysis combining fracture toughness evaluation, flexural strength measurement, fractographic examination and crack configuration modeling. Within this framework, the consideration of processing defects (mainly pores and carbide agglomerates) as stress concentrators acting on an equatorial crack existing around them yields closer agreement between estimated and experimentally determined critical flaw sizes than the simple assumption of these flaws as circular cracks. The length of the referred circumferential crack, an extremely important variable in the model, may be estimated from previous tailoring of the predictive fracture mechanics model. Such calibration is performed through simultaneous implementation of all the experimental data collected (strength, toughness and critical flaw size) as model inputs. The best-fitting results indicate that crack length is intimately associated with key microstructural features of the hardmetal grades, particularly the mean carbide grain size.

Acknowledgments

This work was funded by the Spanish Comisión Interministerial de Ciencia y Tecnología (CICYT) under grant Nº MAT97-0923. The authors are extremely grateful to M. Marsal for her electron microscopy assistance. They would also like to express their gratitude to DURIT Ibérica for kindly supplying all the hardmetal samples used in this investigation. One of the authors (Y.T.) would like to thank the Instituto de Cooperación Iberoamericana (ICI) for the scholarship received. Likewise, another author (D.C.) would like to acknowledge the funding support received from the Generalitat de Catalunya through another scholarship.

REFERENCES

1. Lawn, B. (1993). *Fracture of Brittle Solids.* Second Edition, Cambridge University Press, Cambridge, UK.
2. Rice, R.W. (1984) *J. Mater. Sci.* **19**, 895.
3. Singh, J.P. (1988) *Adv. Ceram. Mater.* **3**, 18.
4. Dusza, J. and Steen, M. (1999) *Int. Mater. Rev.* **44**, 165.
5. Zimmermann, A., Hoffman, M., Flinn, B.D., Bordia, R.K., Chuang,, T.-J., Fuller Jr., E.R. and Rödel, J. (1998) *J. Am. Ceram. Soc.* **81**, 2449.
6. Casellas, D., Alcalá, J., Llanes, L. and Anglada, M. (2000) *J. Mater. Sci.*, submitted for publication.
7. Roebuck, B. and Almond, E.A. (1988) *Int. Mater. Rev.* **33**, 90.
8. Torres, Y. (2000), research in progress.
9. James, M.N., Human, A.M. and Luyckx, S. (1990) *J. Mater. Sci.* **25,** 4810.
10. Torres, Y., Casellas, D., Anglada, M. and Llanes, L. (1999). In: *Proc. of the European Conference on Advances in Hard Materials Production,* pp. 237-244. EPMA, Bellstone, UK.
11. Tada, H., Paris, P.C. and Irwin, G.R. (1973). *The Stress Analysis of Cracks Handbook.* Del Research Corporation, St. Louis, USA.
12. Ravichadran, K.S. (1994) *Acta metall. Mater.* **42,** 143.
13. Kirchner, H.P., Gruver, R.M. and Sotter, W.A. (1976) *Mater. Sci. Eng.* **22,** 147.
14. Baratta, F.I. (1978) *J. Am. Ceram. Soc.* **61,** 490.
15. Kirchner, H.P. and Gruver, R.M. (1979) *J. Mater. Sci.* **14,** 2110.
16. Heinrich, J. and Munz, D. (1980) *Am. Ceram. Soc. Bull.* **59,** 1221.
17. Baratta, F.I. (1982) *J. Am. Ceram. Soc.* **65,** C-32.
18. Heinrich, J. and Munz, D. (1982) *J. Am. Ceram. Soc.* **65,** C-34.

19. Baratta, F.I.. (1981) *J. Am. Ceram. Soc.* **64,** C-3.
20. Fett, T. (1994) *Int. J. Fract.* **67,** R-41.